A Human Depression Circuit Derived From Focal Brain Lesions

Supplementary Information

Table of Contents

Supplementary Methods

Subjects and Lesions

The first dataset (1) consisted of subjects with intracerebral hemorrhage, assessed for depression using the computer adaptive test version of the Neuro Quality of Life scale and NIH Patient Reported Outcomes Measurement Information System (PROMIS) (2). Scores were collected at different time points (28 days, 3 months or 12 months after discharge) for different subjects. The scores are expressed as T scores centered on 50, with a standard deviation of +/- 10. We used an online tool that provides conversions between the Patient Health Questionnaire-9 (PHQ-9), a standard depression scale (3), and raw scores for the Neuro Quality of Life/PROMIS depression subscale. We found that standard thresholds of 4 and 10 for lack of depression and moderate depression on the PHQ-9 were equivalent to Neuro Quality of Life/PROMIS T scores of 50.5 and 59.9, respectively. Thus, we used these cut-offs to classify 10 subjects as depressed (mean = 65.0, standard deviation = 4.7) and 23 subjects as non-depressed (mean = 42.6, standard deviation =5.9) , excluding 18 subjects in the primary analysis. Information on pre-lesion history of depression or anti-depressant medication was not available in this dataset.

The second dataset (4) consisted of subjects with a first symptomatic stroke (ischemic or hemorrhagic) who had clinical evidence of neurological impairment, assessed for depression using the Geriatric Depression Score Short-Form (GDSS) (5) at 3 months and 1 year following stroke. Only the 3 month assessment was used for the current study. For our primary analysis, we classified subjects as "non-depressed" based on GDSS ≤ 5 or "moderate to severe depression" based on GDSS ≥ 11. These cutoffs were based on parameters set by the original authors of the GDSS (5), where GDSS ≥ 11 were classified as 'almost always depression' while those with scores > 5 and < 11 were classified as 'suggestive of depression'. This resulted in 14 subjects with moderate to severe depression (mean GDSS 12.0, standard deviation 1.0) and 73 without depression (mean GDSS 2.2, standard deviation 1.7), while excluding 13 with mild or questionable depression in the primary analysis. The dataset did contain information on pre-lesion history of depression but did not contain information on anti-depressant medication.

The third dataset (6) consisted of subjects with ischemic stroke, assessed three months after stroke with the Patient Health Questionnaire-9 (3). For our primary analysis, we classified subjects as "non-depressed" based on a PHQ-9 score of 4 or less, and "depressed" based on a PHQ-9 score of 10 or greater. These parameters were set by the authors of the PHQ-9 (3). This resulted in 5 subjects with moderate to severe depression (mean PHQ-9 = 13.0, standard deviation = 3.3) and 44 subjects without depression (mean PHQ-9 = 2.1, standard deviation = 1.4), while excluding 14 subjects with mild or questionable depression in the primary analysis. The study excluded subjects with any psychiatric history (including a history of depression) prior to stroke.

The fourth dataset (7) consisted of subjects with a first ischemic or intracerebral hemorrhagic stroke, evaluated for depression one month after stroke using the Hospital Anxiety and Depression Scale (HADS) (8). Those with a score of 11 or higher were evaluated with the Mini-International Neuropsychiatric Interview (MINI), a semi-structured

clinical interview (9), to determine presence of either major depression (major depressive-like episode following stroke) or minor depression (depressive features following stroke) per DSM-IV criteria. For our primary analysis, we classified subjects as "non-depressed" or "major depression" based on a previously published categorization of this dataset (7). This resulted in 7 subjects with major depression and 38 controls, excluding 6 individuals that were classified by the original authors as having 'minor depression' in the primary analysis. The dataset did contain information on pre-lesion history of depression. Three subjects included in our analysis were on antidepressant medication at the time of evaluation: one subject was a control, and the other two were classified as having 'minor depression' in the original dataset (equivalent to 'mild or questionable depression' in our analysis).

The fifth dataset (10) consisted of Vietnam War veterans with penetrating traumatic brain injury, assessed with the Beck Depression Inventory II about 33-39 years following their injury (11). For our primary analysis we classified subjects as "non-depressed" based on a BDI-II score ≤ 8 and "moderate to severe depression" based on a BDI-II score ≥ 20. These cutoffs were the same values used in prior analyses of this dataset (10). This resulted in 22 depressed subjects (mean BDI score 29.9, standard deviation 5.6), and 122 non-depressed subjects (mean BDI score 3.6, standard deviation 2.4), excluding 52 subjects with mild or questionable depression (BDI range 9-19) in the primary analysis. The dataset did not have information on pre-lesion history of depression or anti-depressant medication (10).

In total, the primary analysis dataset, which used a binary representation of depression status (depressed versus non-depressed), included 358 lesions. For analyses involving depression as a continuous measure, we included the 103 previously excluded subjects with mild or questionable depression (total N = 461). Depression scores within each dataset (NeuroQOL, GDSS, PHQ-9, HADS, BDI-II) were converted to z-scores (zero mean unit variance) to allow for cross-dataset analyses.

In analyses involving depression as a continuous measure, no subjects were excluded, retaining a total of 461 subjects.

Analysis of Lesion Location

To identify any lesioned voxel significantly associated with depression, we performed voxel lesion symptom mapping (VLSM) using NiiStat, a Matlab software package (https://github.com/neurolabusc/NiiStat) that can control for covariates (12).

NiiStat performs a pooled-variance t-test using general linear regression. For VLSM with NiiStat in our binary dataset, a total of 358 depression and control lesions were compared for voxels occurring in at least 5% of lesions, controlling for lesion size and dataset as nuisance regressors, with Freedman-Lane permutation for significance testing set at $p < 0.025$ one-tailed (equivalent to $p < 0.05$ two-tailed). The default setting of 2000 permutations was used. These parameters and statistical cutoffs were chosen based on published recommendations for VLSM analysis (13, 14). We performed this analysis using the Harvard-Oxford bilateral middle frontal gyrus (cutoff probability > 0%) as a mask.

We repeated the analysis using two DLPFC masks from prior lesion analyses ((10, 15); see below and Supplementary Figure 2), and using no mask at all (whole brain). The two DLPFC masks from prior lesion analyses consisted of the left anterior frontal region (Robinson *et al*, 1984) and the bilateral dorsolateral prefrontal region (Koenigs *et al*, 2008) (see Supplementary Figure 2, Supplementary Table 2). We then conducted this analysis with depression as a continuous measure and the entire dataset (461 subjects), again using the Harvard-Oxford bilateral middle frontal gyrus as a mask, then the two DLPFC masks from prior lesion analyses, and then no mask at all (see Supplementary Table 2).

We then replicated the prior lesion analyses of Robinson *et al* (15) and Koenigs *et al* (10) using their respective anatomical definitions and statistical methods in our binary dataset (N = 358). First, we used the definition of Robinson et al (15) to classify lesions according to where they fell with respect to certain percentages of the anterior-posterior (AP) distance: "The lesion was anterior if the anterior border of the lesion was rostral to 40 per cent of the AP distance and the posterior border was anterior to 60 per cent of the AP distance. On the other hand, a lesion was posterior if its anterior border was posterior to 40 per cent of the AP distance and the posterior border was caudal to 60 per cent of the AP distance." Lesions not fulfilling criteria for being either anterior or posterior were excluded. Chi-squared tests with Yates' continuity correction for statistical significance were performed to assess whether there was a difference in prevalence of depression between left anterior and left posterior lesions, between left anterior and right anterior lesions, or between right anterior and right posterior lesions.

Next, we replicated the analyses of Koenigs et al, 2008 (10) in our binary dataset (N=358). We classified lesions as bilateral dorsolateral prefrontal lesions, bilateral ventromedial prefrontal lesions, or non-prefrontal, while excluding unilateral vmPFC or dlPFC lesions: "The vmPFC ROI was defined as those areas of PFC inferior to $z = 0$ and medial to $x = 20$ and $x = -20$… The dlPFC ROI was defined as those areas of PFC superior to $z = 0$ and lateral to $x = -10$ and $x = 10$. A patient was included in the vmPFC group if his lesion occupied vmPFC in both hemispheres, but did not occupy any portion of dlPFC in either hemisphere. A patient was included in the dorsal PFC group if his lesion occupied dlPFC in both hemispheres, but did not occupy any portion of vmPFC in either hemisphere." We used Fisher's exact test to assess whether there was a significant difference in the proportion of depression among individuals with bilateral dlPFC lesions versus individuals with bilateral vmPFC lesions and versus non-prefrontal lesions.

Finally, we performed additional lesion laterality analyses. First, we created masks for each hemisphere by combining the Harvard Oxford cerebral cortex and cerebral white matter masks for each hemisphere, available in FSL 3.2.0. We then used these masks to classify lesions according to whether any voxels within them fell into the left cerebral hemisphere but not the right cerebral hemisphere, the right cerebral hemisphere but not the left, both, or neither. A chi-squared test with Yates' continuity correction for statistical significance was performed to assess whether there was a difference in prevalence of depression between left and right-sided lesions (excluding those lesions that fell into both or neither region).

Next, we used the Harvard Oxford middle frontal gyrus region of interest to create regions of interest representing the left and right middle frontal gyrus. We classified lesions according to whether any voxels within them fell into left middle frontal gyrus but not the right middle frontal gyrus, the right middle frontal gyrus but not the left middle frontal gyrus, both, or neither. A chi-squared test with Yates' continuity correction for statistical significance was performed to assess whether there was a difference in prevalence of depression between left middle frontal gyrus and right middle frontal gyrus lesions (excluding those lesions that fell into both or neither region).

Lesion Network Mapping

As described in the main text, we used each lesion image as a seed in a whole brain functional connectivity analysis in a normative dataset of 1000 subjects from the Brain Genomics Superstruct Project (https://dataverse.harvard.edu/dataverse/GSP) on whom resting state functional connectivity had been obtained using a 3T MRI. Processing of these scans has been fully described elsewhere (16), and included correction for motion and non-specific variance using global signal regression. To create a lesion network map, time series for voxels within the lesion were correlated with the time series from all other brain voxels in each of the 1000 healthy control subjects. Results were statistically combined across the 1000 subjects to create a voxelwise map of T values representing the strength and consistency of functional connectivity for each lesion location (Figure 2). Positive functional connectivity refers to a positive (direct) correlation of BOLD timeseries between regions or voxels, while negative functional connectivity refers to a negative (inverse) correlation of BOLD timeseries between regions or voxels.

Lesion network maps of 58 depressed versus 300 non-depressed subjects were statistically compared using a general linear model and permutation testing (Permutation Analysis of Linear Models in FSL 3.2.0), including lesion size and dataset as covariates (17, 18), and using the Harvard Oxford bilateral middle frontal gyrus (cutoff probability > 0%) as a mask. This region is provided in the Harvard-Oxford Cortical Atlas in FSLview version 3.2.0. We used a conservative voxel-level family-wise error correction for multiple comparisons, correcting for all brain voxels ($p < 0.05$). This is more stringent than the commonly used cluster-based correction which has been associated with false positives (19). We repeated this analysis with no mask and with two *a priori* DLPFC ROIs from the literature (Supplementary Figure 2) that we used in our analysis of lesion location, described in the previous section.

The significant results within the Harvard Oxford bilateral middle frontal gyrus mask were extracted as a seed, and the functional connectivity of this seed to the rest of the brain was computed using the normative connectome of 1000 healthy subjects. The resulting network map, which we term the "depression circuit", by definition encompasses lesion locations associated with depression while excluding lesion locations not associated with depression (peaks reported in Supplementary Table S3).

We then generated depression circuits from lesions only within each etiology (N = 52 for hemorrhagic stroke, N = 162 for ischemic stroke, and N=144 for penetrating traumatic brain injury). Following a similar process, we compared lesion network maps of depressed and non-depressed subjects within each etiology using a general linear model and permutation testing, including lesion size as a covariate, and using the Harvard-Oxford bilateral middle frontal gyrus as a mask. Due to loss of power in the smaller within-etiology sample sizes, results did not survive voxel-wise multiple comparison correction. Thus, different thresholds were used to define each DLPFC ROI. Seeds were generated by thresholding the uncorrected results at $p = 0.05$ (hemorrhagic lesions), $p = 0.001$ (ischemic lesions), and $p = 0.01$ (penetrating traumatic brain injury lesions). The functional connectivity of these seeds to the rest of the brain was computed using the normative connectome of 1000 subjects to generate depression circuits for each etiology. The spatial correlation of each depression circuit with the main depression circuit was assessed using a Pearson's correlation of the intensity at each voxel (Supplementary Figure S3).

An identical process was followed to generate a depression circuit from lesions of subjects with reported lack of history of depression prior to their lesion (N=168, of which N=24 depressed and N=144 non-depressed), using dataset and lesion size as covariates. Results of the comparison of lesion network maps of depressed and non-depressed individuals were thresholded at $p = 0.005$ uncorrected to generate a seed (Supplementary Figure S4A) that was then used to generate the depression circuit (Supplementary Figure S4B) using the normative connectome. The spatial correlation of this depression circuit with the primary depression circuit was assessed using a Pearson's correlation of the intensity at each voxel.

Leave-one-out Validation and Network Damage Scores

To ensure that our findings were not biased by any one of our five datasets, we performed a leave-one-dataset-out validation method. We statistically compared the lesion network maps of depressed and control subjects five times, each time leaving out one of the five datasets. For example, one of these five analyses used subjects in datasets 2-5 and excluded subjects in dataset 1, while another used subjects in datasets 1-4 and excluded subjects dataset 5. Each time, voxels that survived voxel-wise FWE correction were extracted as seeds for generating depression circuits (Figure 3A).

Then, we computed the functional connectivity of each of these seeds to the rest of the brain using the normative connectome data of 1000 subjects. Thus, we generated five network maps representing the circuitry of lesion-associated depression (Figure 3B and 3C), which we term 'depression circuits'. The spatial correlation between each pair of these maps was calculated as a Pearson's correlation between the intensities of all voxels in the maps.

We then assigned each subject a 'network damage score' using the depression circuit that was generated while excluding the dataset to which the subject belonged (Figure 3B and 3C). For example, network damage scores for subjects in Dataset 1 were assigned using the depression circuit that was created from Datasets 2-5. Each subject's

network damage score was calculated by summing the intensity values (T values) of those voxels in the depression circuit that overlapped with that subject's lesion. We regressed this score against lesion size and dataset and extracted the residuals to create an adjusted network damage score, which was used in all analyses.

Due to the non-normality of the network damage score, statistical significance for all analyses using this score was calculated using permutation testing. We examined whether the network damage score differed between depressed and control subjects using a permutation equivalent of a t-test (test of difference of means) (Figure 3D). We also assessed whether network damage score predicted depression using logistic regression. Analyses on the full cohort of subjects (N = 461) using a continuous measure of depression are described fully in the main text. Permutation testing was used for statistical significance due to non-normality of both the network damage score and the continuous depression measure.

Finally, we assessed whether lesion size alone predicted depression in these models. Lesion size was used as a predictor of binary depression status using a logistic regression model in the binary dataset (N=358), and as a predictor of continuous depression score using a Pearson's correlation in the continuous dataset (N=461).

Analyses dividing subjects into risk categories based on network damage score are described fully in the main text.

To set statistical significance using permutations, assignments of depressed or non-depressed status (or assignment of continuous depression measure) to subjects were randomly shuffled to create one million datasets. The test statistic of the correlation was calculated in all datasets to create a distribution of test statistics. The p value was the proportion of test statistics that were greater than the actual test statistic in our data.

Post-stroke Depression Treatment Targets

To identify studies of transcranial magnetic stimulation for post-stroke depression, we searched PubMed using the following search terms: "stroke", "depression" and "transcranial magnetic stimulation". This search yielded 113 English-language articles, whose abstracts we perused to identify 5 studies that successfully used transcranial magnetic stimulation with a primary endpoint of treating post-stroke depression in at least three subjects and provided adequate detail on the location of stimulation. We then identified the coordinates of the stimulation locations used in each of these studies. Two studies used 5 cm anterior to the motor hotspot ((20, 21), MNI coordinates: x = -41, y = 16, z = 54; coordinates obtained from (22)). Two studies (23, 24) used the left F3 electrode on the 10/20 EEG coordinate system (MNI coordinates: x = -37, y = 26, z = 49; coordinates obtained from (22)). The fifth study (25) used an approximation of the center of the middle frontal gyrus. To approximate the coordinates of that location, we identified the surface peak of the left Harvard Oxford middle frontal gyrus using the viewing software FSLeyes, within FSL 3.2.0 (MNI coordinates: x = -42, y = 20, z = 52). As a control, we used the vertex (Cz on EEG), frequently used as a control stimulation location in transcranial magnetic stimulation trials (coordinates: x = 1, y = -15, z = 74; (26)).

We created four 12-mm cone regions of interest (ROIs) centered on these stimulation locations by following previously published methodology (27). To summarize this methodology, concentric spheres were created with a radius of 2 mm, 4 mm, 7 mm, 9 mm, and 12 mm, centered on the coordinates of each stimulation location. The resulting structure was masked against the MNI 152 brain.

Using the normative connectome of 1000 subjects, we computed the resting state functional connectivity between the results of our lesion network mapping analysis (i.e., the region in the left DLPFC, 'LNM' in Figure 2B) and each cone ROI. This generated an r value representing the connectivity of each cone ROI with the results of our lesion network mapping analysis. We then compared the r value for each of the three successful stimulation targets with the r value for the vertex (a known 'unsuccessful' treatment target) using Hotelling's t-test and the cocor statistical package (28).

Supplementary Tables and Figures

Mask	N	Depression measure	# voxels analyzed	P value
Harvard-Oxford Middle Frontal Gyrus (bilateral)	358	binary	236	n.s.
Koenigs et al, 2008	358	binary	2291	n.s.
Robinson et al, 1984	358	binary	827	n.s.
No mask (whole brain)	358	binary	5917	n.s.
Harvard-Oxford Middle Frontal Gyrus (bilateral)	461	continuous	200	n.s.
Koenigs et al, 2008	461	continuous	3363	n.s.
Robinson et al, 1984	461	continuous	2113	n.s.
No mask (whole brain)	461	continuous	8386	n.s.

Supplementary Table S1. Voxel-based lesion-symptom mapping using NiiStat. Analyses regarding lesion location were performed in both the binary dataset (N=358), which excluded subjects with mild or questionable depression and used a binary variable to represent depressed or non-depressed status, and the continuous dataset, which included all subjects and used a continuous variable to represent depression severity.

	Left hemisphere	**Right hemisphere**	**Both**	**Neither**	**Total (%)**
Not depressed	91	101	88	20	300
Depressed	18	21	19	0	58
N (% of lesions)	109 (30%)	122 (34%)	107 (30%)	20 (6%)	358 (100%)
	Left MFG	**Right MFG**	**Both**	**Neither**	
Not depressed	31	53	8	208	300
Depressed	9	9	4	36	58
N (% of lesions)	40 (11%)	62 (17%)	12 (3%)	244 (68%)	358 (100%)

Supplementary Table S2. Lesion laterality in the binary (N=358) sample. Lesions were classified according to whether any voxels within them fell into the left cerebral hemisphere but not the right hemisphere, the right cerebral hemisphere but not the left, both, or neither (top four lines of table). They were also classified according to whether any voxels within them fell within the left middle frontal gyrus (MFG) but not the right, the right MFG but not the left, both, or neither (bottom four lines of table). There was no significant difference in prevalence of depression between lesions involving the left MFG and the right MFG, or between lesions involving the left and right cerebral hemispheres ($p > 0.05$).

Cluster	Location	Max T	Max X	Max Y	Max Z
1	Left middle frontal gyrus (left DLPFC)	207	-32	12	34
2	Right cerebellum	37	12	-74	-28
3	Right middle frontal gyrus (right DLPFC)	36	48	24	28
4	Lateral occipital cortex	36	-32	-70	48

Supplementary Table S3. Peaks of clusters within the depression circuit. Peaks were identified by thresholding the depression circuit at the lowest value that generated more than two clusters (T=36). Four clusters were generated, and the peaks of each are listed in this table.

Dataset	**1. Excluding Naidech et al, 2016**	**2. Excluding Corbetta et al, 2015**	**3. Excluding Egorova et al, 2018**	**4. Excluding Gozzi et al, 2004**	**5. Excluding Koenigs et al, 2008**
1. Excluding Naidech et al, 2016	1	0.84	0.97	0.98	0.96
2. Excluding Corbetta et al, 2015		1	0.92	0.85	0.78
3. Excluding Egorova et al, 2018			1	0.96	0.90
4. Excluding Gozzi et al, 2004				1	0.91
5. Excluding Koenigs et al, 2008					1

Supplementary Table S4. R values of Pearson's correlations between pairs of depression circuits. All five of our leave-one-dataset-out analyses yielded similar regions in the left DLPFC that survived voxel-level FWE correction. The connectivity of these regions to the rest of the brain was examined using a normative connectome of 1000 healthy subjects, generating five depression circuits representing lesion-associated depression. These five depression circuits were highly spatially correlated, as indicated by the high Pearson's correlations between any given pair of network maps.

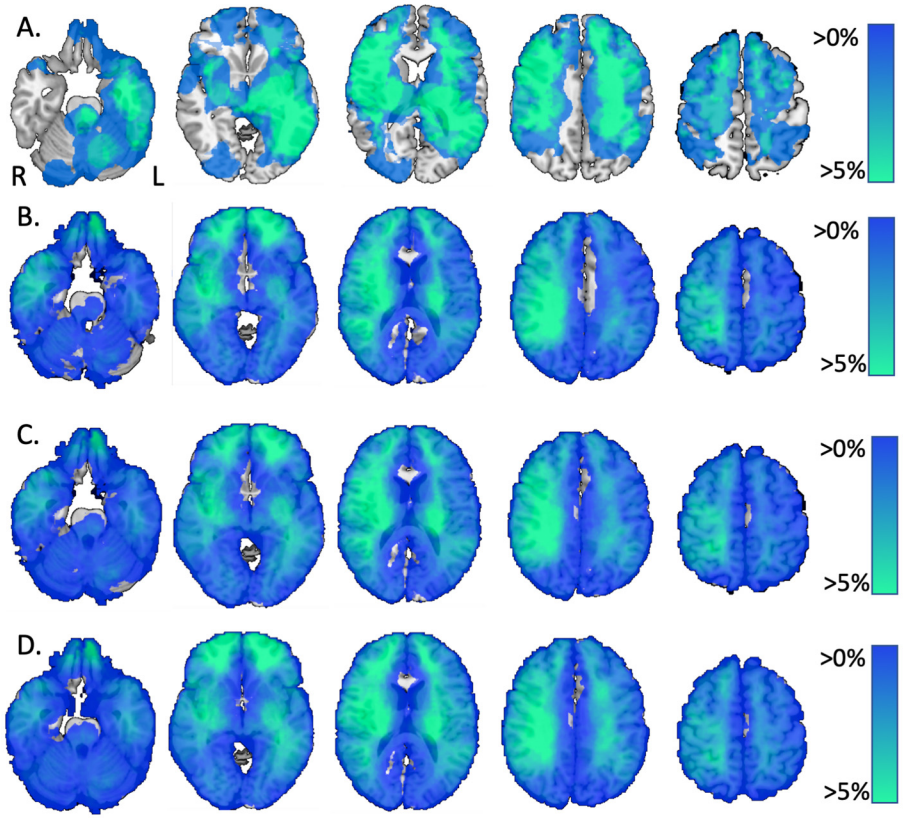

Supplementary Figure S1. **Lesion overlap maps, thresholded at 0 %.** Lesions were overlapped (summed) to depict the number of lesions overlapping at any given location.
A. Overlap map of lesions belonging to depressed subjects (N=58), max = 8.
B. Overlap map of lesions belonging to control subjects (N=300), max = 26.
C. Overlap map of depression and control lesions (excluding subjects with mild or questionable depression, N = 358), max = 32.
D. Overlap map of all lesions (N=461), max = 40.
Slice location: Z= -25, -5, 15, 35, 55

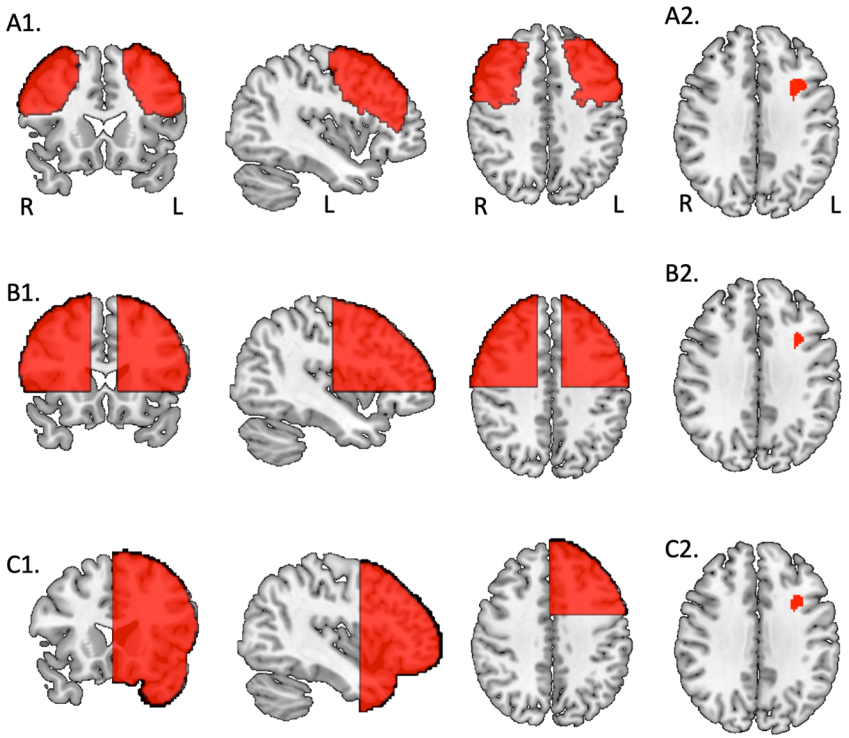

Supplementary Figure S2. A1. Harvard Oxford bilateral middle frontal gyrus (x=40, y=20, z=40).
A2. Results of general linear model comparing lesion network maps of depressed and control subjects, masking to Harvard Oxford Middle Frontal Gyrus (voxels with probability > 0%), with voxel-level FWE correction. Voxels in red survived multiple comparison correction (peak: T = 4.37, p_c = 0.0050, coordinates x = -32, y = 12, z = 36).
B1. Koenigs ROI (x=40, y=20, z=40) from Koenigs et al, 2008. B2. Results of general linear model comparing lesion network maps of depressed and control subjects, masking to Koenigs DLPFC, with voxel-level FWE correction. Voxels in red survived multiple comparison correction (peak: T = 4.37, p_c = 0.013, coordinates x = -32, y = 12, z = 36).
C1. Robinson ROI (x=40, y=20, z=40) from Robinson et al, 1984. C2. Results of general linear model comparing lesion network maps of depressed and control subjects, masking to Robinson ROI, with voxel-level FWE correction. Voxels in red survived multiple comparison correction (peak: T = 4.37, p_c = 0.0096; x = -32, y = 12, z = 36).

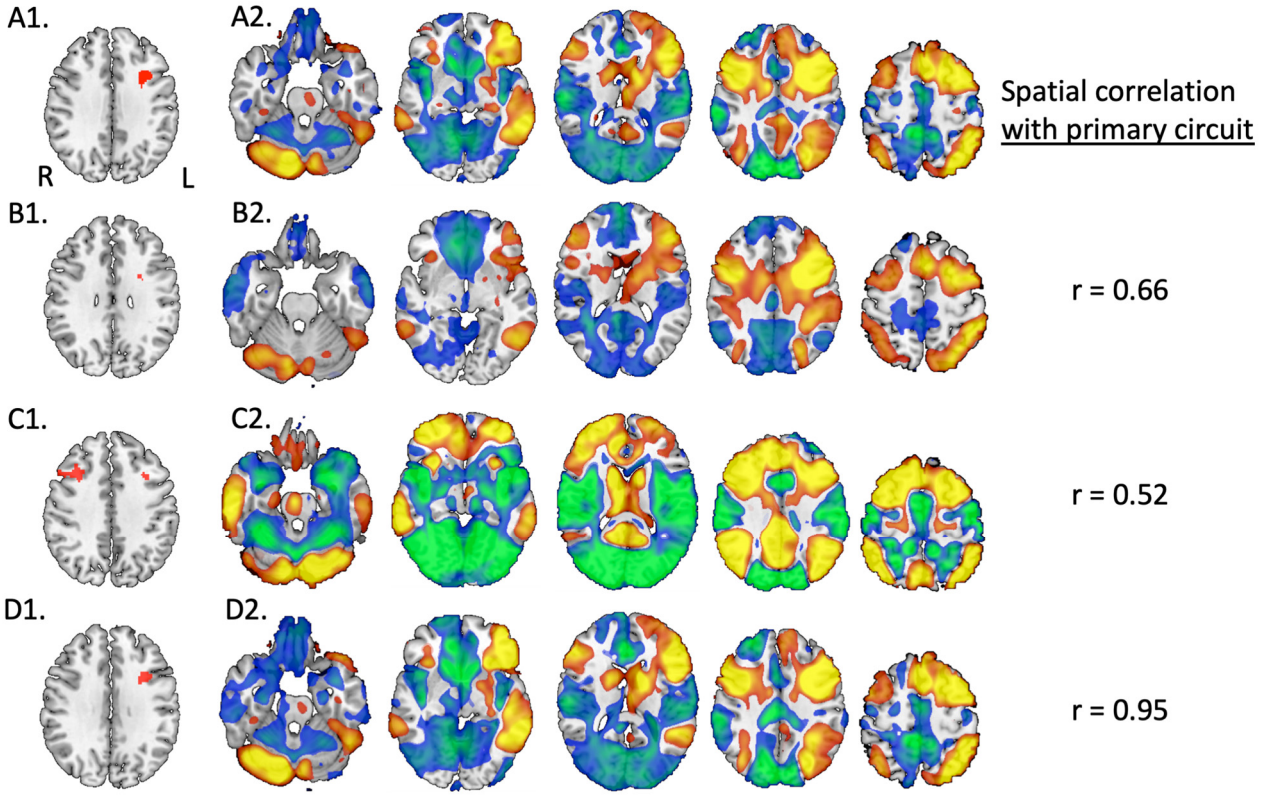

Supplementary Figure S3. Depression circuit compared to within-etiology depression circuits.
A1. 'Seed' used to generate depression circuit in primary analysis.
A2. Primary depression circuit generated using lesions of all etiologies (N = 358).
B1. Seed' used to generate depression circuit for hemorrhagic lesions.
B2. Depression circuit generated from hemorrhagic lesions (N = 52).
C1. Seed' used to generate depression circuit for ischemic lesions.
C2. Depression circuit generated from ischemic lesions (N = 162).
D1. Seed' used to generate depression circuit for penetrating traumatic brain injury lesions.
D2. Depression circuit generated from penetrating traumatic brain injury lesions (N=144).
z = -25, -5, 15, 35, 55 for slices of circuits. Thresholds for generating seeds are described in Supplementary Methods.

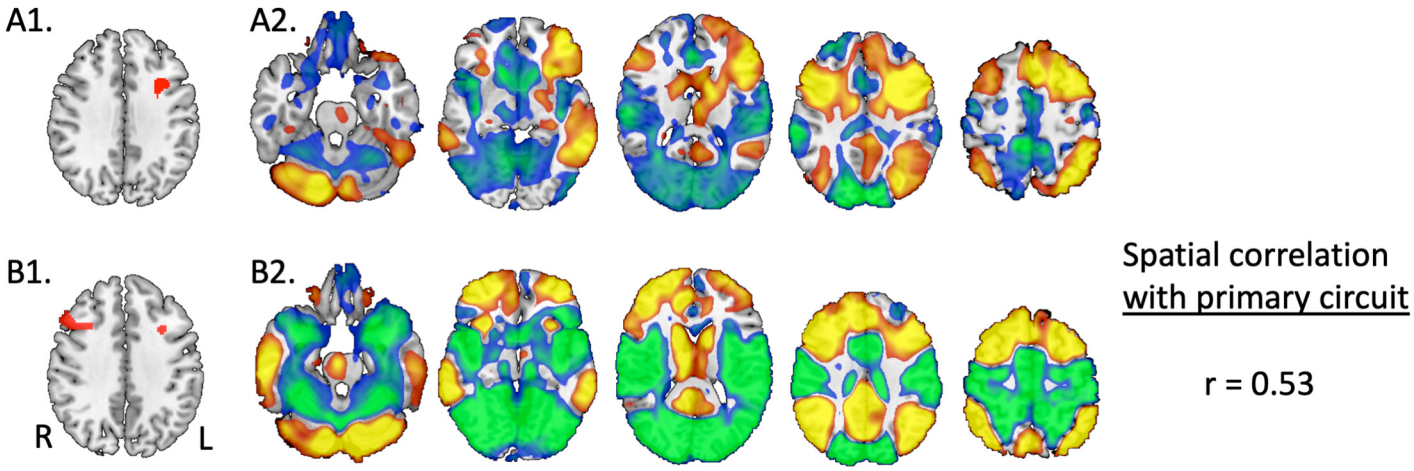

Supplementary Figure S4. Depression circuit compared to circuit of subjects (N=358) with confirmed lack of history of depression prior to lesion (N=168).
A1. Region of interest used as 'seed' to generate depression circuit in primary analysis.
A2. Axial slices of primary depression circuit at z = -25, -5, 15, 35, 55.
B1. Region of interest used as 'seed' to generate depression circuit for subset of subjects with confirmed lack of history of depression prior to lesion (N=168). Seed was generated by comparing lesion network maps of depressed and non-depressed subjects in PALM using a general linear model and thresholding the results at p (uncorrected) = 0.005.
B2. Axial slices of depression circuit generated from subjects with confirmed lack of history of depression prior to lesion (z = -25, -5, 15, 35, 55).

Supplementary References

1. Naidech AM, Polnaszek KL, Berman MD, Voss JL (2016): Hematoma Locations Predicting Delirium Symptoms After Intracerebral Hemorrhage. *Neurocrit Care*. 24:397-403.

2. Gershon RC, Lai JS, Bode R, Choi S, Moy C, Bleck T, et al. (2012): Neuro-QOL: quality of life item banks for adults with neurological disorders: item development and calibrations based upon clinical and general population testing. *Quality of life research : an international journal of quality of life aspects of treatment, care and rehabilitation*. 21:475-486.

3. Kroenke K, Spitzer RL, Williams JB (2001): The PHQ-9: validity of a brief depression severity measure. *J Gen Intern Med*. 16:606-613.

4. Corbetta M, Ramsey L, Callejas A, Baldassarre A, Hacker CD, Siegel JS, et al. (2015): Common behavioral clusters and subcortical anatomy in stroke. *Neuron*. 85:927-941.

5. Burke WJ, Roccaforte WH, Wengel SP (1991): The short form of the Geriatric Depression Scale: a comparison with the 30-item form. *J Geriatr Psychiatry Neurol*. 4:173-178.

6. Egorova N, Cumming T, Shirbin C, Veldsman M, Werden E, Brodtmann A (2018): Lower cognitive control network connectivity in stroke participants with depressive features. *Transl Psychiatry*. 7:4.

7. Gozzi SA, Wood AG, Chen J, Vaddadi K, Phan TG (2014): Imaging predictors of poststroke depression: methodological factors in voxel-based analysis. *BMJ Open*. 4:e004948.

8. Zigmond AS, Snaith RP (1983): The hospital anxiety and depression scale. *Acta Psychiatr Scand*. 67:361-370.

9. Sheehan DV, Lecrubier Y, Sheehan KH, Amorim P, Janavs J, Weiller E, et al. (1998): The Mini-International Neuropsychiatric Interview (M.I.N.I.): the development and validation of a structured diagnostic psychiatric interview for DSM-IV and ICD-10. *J Clin Psychiatry*. 59 Suppl 20:22-33;quiz 34-57.

10. Koenigs M, Huey ED, Calamia M, Raymont V, Tranel D, Grafman J (2008): Distinct regions of prefrontal cortex mediate resistance and vulnerability to depression. *J Neurosci*. 28:12341-12348.

11. Beck AT, Steer RA, Brown G (1996): Manual for the Beck Depression Inventory-II. San Antonion, TX: Psychological Corporation.

12. Stark BC, Yourganov G, Rorden C (2018): User Manual and Tutorial for NiiStat. http://wwwnitrcorg/projects/niistat.

13. Karnath HO, Sperber C, Rorden C (2018): Mapping human brain lesions and their functional consequences. *Neuroimage*. 165:180-189.

14. Sperber C, Karnath HO (2017): Impact of correction factors in human brain lesion-behavior inference. *Hum Brain Mapp*. 38:1692-1701.

15. Robinson RG, Kubos KL, Starr LB, Rao K, Price TR (1984): Mood disorders in stroke patients. Importance of location of lesion. *Brain*. 107 (Pt 1):81-93.

16. Yeo BT, Krienen FM, Sepulcre J, Sabuncu MR, Lashkari D, Hollinshead M, et al. (2011): The organization of the human cerebral cortex estimated by intrinsic functional connectivity. *J Neurophysiol*. 106:1125-1165.

17. Winkler AM, Ridgway GR, Webster MA, Smith SM, Nichols TE (2014): Permutation inference for the general linear model. *Neuroimage*. 92:381-397.

18. The MathWorks I (2015): MATLAB and Statistics Toolbox Release 2015b. Natick, Massachusetts.

19. Eklund A, Nichols TE, Knutsson H (2016): Cluster failure: Why fMRI inferences for spatial extent have inflated false-positive rates. *Proc Natl Acad Sci U S A*. 113:7900-7905.

20. VanDerwerker CJ, Ross RE, Stimpson KH, Embry AE, Aaron SE, Cence B, et al. (2018): Combining therapeutic approaches: rTMS and aerobic exercise in post-stroke depression: a case series. *Top Stroke Rehabil*. 25:61-67.

21. El Etribi A, El Nahas N, Nagy N, Nabil H (2010): Repetitive transcranial magnetic stimulation in post stroke depression. *Current Psychiatry*. 17:9-14.

22. Fox MD, Buckner RL, White MP, Greicius MD, Pascual-Leone A (2012): Efficacy of transcranial magnetic stimulation targets for depression is related to intrinsic functional connectivity with the subgenual cingulate. *Biol Psychiatry*. 72:595-603.

23. Gu SY, Chang MC (2017): The Effects of 10-Hz Repetitive Transcranial Magnetic Stimulation on Depression in Chronic Stroke Patients. *Brain stimulation*. 10:270-274.

24. Kim BR, Kim DY, Chun MH, Yi JH, Kwon JS (2010): Effect of repetitive transcranial magnetic stimulation on cognition and mood in stroke patients: a double-blind, sham-controlled trial. *Am J Phys Med Rehabil*. 89:362-368.

25. Jorge RE, Robinson RG, Tateno A, Narushima K, Acion L, Moser D, et al. (2004): Repetitive transcranial magnetic stimulation as treatment of poststroke depression: a preliminary study. *Biol Psychiatry*. 55:398-405.

26. Okamoto M, Dan H, Sakamoto K, Takeo K, Shimizu K, Kohno S, et al. (2004): Three-dimensional probabilistic anatomical cranio-cerebral correlation via the international 10-20 system oriented for transcranial functional brain mapping. *Neuroimage*. 21:99-111.

27. Fox MD, Liu H, Pascual-Leone A (2013): Identification of reproducible individualized targets for treatment of depression with TMS based on intrinsic connectivity. *Neuroimage*. 66:151-160.

28. Diedenhofen B, Musch J (2015): cocor: a comprehensive solution for the statistical comparison of correlations. *PLoS One*. 10:e0121945.